

Correlation effects for chiral semiconducting single wall carbon nanotube: a density matrix renormalization group study

Fei Ye,¹ Bing-Shen Wang,² Jizhong Lou,³ and Zhao-Bin Su³

¹Center for Advanced Study, Tsinghua University, Beijing 100084, China

²State Key Laboratory of Semiconductor Superlattice and Microstructure and Institute of Semiconductor, Academia Sinica, Beijing 100083, China

³Institute of Theoretical Physics, Academia Sinica, Beijing 100080, China

In this paper, we report the applicability of the density matrix renormalization group(DMRG) approach to the cylindrical single wall carbon nanotube (SWCN) for purpose of its strong correlation effect. By applying the DMRG approach to the $t+U+V$ model, with t and V being the hopping and Coulomb energies between the nearest neighboring sites, respectively, and U the onsite Coulomb energy, we calculate the phase diagram for the SWCN with chiral numbers ($n_1 = 3, n_2 = 2$), which reflects the competition between the correlation energy U and V . Within reasonable parameter ranges, we investigate possible correlated ground states, the lowest excitations and the corresponding correlation functions in which the connection with the excitonic insulator is particularly addressed.

PACS numbers: 71.10.Fd, 71.10.Hf, 71.35.-y, 78.67.Ch

Since the discovery of carbon nanotube, many efforts, both experimental and theoretical, have been put into understanding the electron correlation effect, specially for thin single wall carbon nanotubes(SWCN). The transport as well as the angle-integrated photoemission[1, 2]studies on the bundles of SWCN show interesting evidence of the non-trivial correlation effects which are believed to be contributed by the metallic SWCNs and are consistent with the Tomonaga-Luttinger theory[3, 4, 5]. For the semiconducting SWCNs, the discrepancy between the experimentally measured ratio of the absorption frequency to the emission frequency[6, 7] and that predicted by the tight binding approximation(TBA)[14] is also attributed to the correlation effects in literatures[8, 9, 10]. Theoretically, the correlation effect of SWCNs so far has been treated[3, 4, 5, 8, 9, 10, 11, 12, 13] by *ab initio* numerical calculations, perturbative renormalization group(RG), and various improved or modified Hartree-Fock approximations(HFA). However none of the existing approaches can handle the strong correlation effects in the SWCNs seriously.

It is known that the π -electron has its wave function extending along the radial direction of the SWCN[14], with a weak overlap among themselves, so that its kinetic energy in a range of 2.4-3.2eV is much smaller than the onsite Coulomb energy about 11.76eV[15] while the nearest neighboring (n.n.) Coulomb energy is also as big as an order of 5eV. Therefore the SWCN is truly a strongly correlated electronic system. The minimal model Hamiltonian for a gapped intrinsic semiconducting SWCN would be

$$H = \sum_{\langle i,j \rangle} c_{i,\sigma}^\dagger c_{j,\sigma} + h.c. + U \sum_i n_{i,\uparrow} n_{i,\downarrow} + V \sum_{i,j} (n_i - 1)(n_j - 1), \quad (1)$$

where the hopping energy t is set to be unit, while U and

V are on site and n.n. Coulomb energies, respectively. c_i and c_i^\dagger are the electron annihilation and creation operators with i as the site index, respectively. The particle number operator for spin σ at site i is $n_{i,\sigma} = c_{i,\sigma}^\dagger c_{i,\sigma}$ and $n_i = n_{i,\uparrow} + n_{i,\downarrow}$. Here we neglect the curvature induced difference among the three hopping directions on each site. We notice that this model has been studied in Refs.[4, 13] for metallic tubules by perturbative RG and unrestricted HFA, respectively. It has also been applied to the graphite system[16].

In this paper, we report the applicability of the DMRG approach to the cylindrical SWCN for purpose of studying its strong correlation effect. By applying this approach to the $t+U+V$ model Eq.(1), we compute the phase diagram for the SWCN with chiral numbers ($n_1 = 3, n_2 = 2$), which essentially reflects the competition between the correlation energies U and V . Within reasonable parameter ranges of U/t and V/t , we investigate possible correlated ground states, the lowest excitations and the corresponding correlation functions.

As it is well accepted the DMRG approach is an accurate and efficient treatment for the quasi-1D strongly correlated systems[17]. The main problem for the implementation of DMRG to the SWCN lies in how to construct an appropriate super block configuration for such a cylindrically warped hexagonal lattice sheet. We notice that, following the literature[18], for a given pair of chiral numbers (n_1, n_2) with N as their greatest common divisor, the corresponding SWCN can be reconstructed by successive piling of motifs along the tubule axis conducted by a screw operation[18], where each motif contains N unit cells in coincidence with the N -fold rotational symmetry of the tubule and it forms an N -multiple helical structure. The motif cells are labelled by two integers (m, l) with $l = 1, 2, \dots, N$ which corresponds the l -th cell in the m -th motif, an index ν is also introduced to distinguish the two carbon atoms $\nu = A, B$ in the same unit

cell. Based upon the above observation, we map such N -multiple helical structure, i.e., the SWCN, onto a $2N$ chain lattice so as to make the DMRG procedure can be straightforwardly implemented. The $2N$ lattice chains are labelled by l, ν while the motif index m is mapped onto the site index in each of the $2N$ chains. As a result, the three n.n. of the site (m, l, A) now have the site labels as (m, l, B) , $(m - \frac{n_1}{N}, l + p_1, B)$, $(m + \frac{n_2}{N}, l - p_2, B)$, where p_1, p_2 are integer solutions of equation $n_1 p_2 - n_2 p_1 = N$. In particular, for case of $N = 1$, which is the most advantaged, all the motif cells on the tubule can be threaded by only one helical curve and l becomes a dummy index. Then the Hamiltonian in Eq.(1) can be rigorously mapped to a twisted two-chain model with finite long range hoppings as $H = H_t + H_U + H_V$ with

$$\begin{aligned} H_t &= \sum_{m, \mu \in \mathcal{S}} \sum_{\sigma} c_{m, \sigma}^{A\dagger} c_{m+\mu, \sigma}^B + h.c. \\ H_U &= U \sum_{m, \nu=A, B} n_{m, \uparrow}^{\nu} n_{m, \downarrow}^{\nu} \\ H_V &= V \sum_{m, \mu \in \mathcal{S}} (n_m^A - 1)(n_{m+\mu}^B - 1) \end{aligned} \quad (2)$$

where $\mathcal{S} = \{0, -n_1, n_2\}$, $n_{m, \sigma}^{\nu} = c_{m, \sigma}^{\nu\dagger} c_{m, \sigma}^{\nu}$, $n_m^{\nu} = n_{m, \uparrow}^{\nu} + n_{m, \downarrow}^{\nu}$ and $c_{m, \sigma}^{\nu}$ is exactly the same operator $c_{i, \sigma}$ but with its index relabelled in terms of motif-cell labels. Fig.(1a) and (1b) show such a mapping for the tubule ($n_1 = 3, n_2 = 2$) with $N = 1$. To extract most physi-

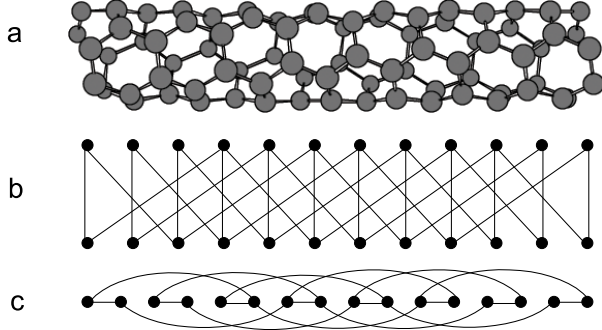


FIG. 1: Illustration for the mapping from a cylindrical SWCN(1a) with index (3,2) to a twisted two chain model with finite long range hopping (1b), where the solid lines connect the n.n. pairs. For purpose of DMRG calculation, we further squeeze the two chains in (1b) into a single chain (1c) with A atom and B atom arranged alternatively, where the lines are kept with the same meaning as in (1b).

cal implications with small enough computing effort, in this paper, we apply the DMRG approach to the intrinsic SWCN with ($n_1 = 3, n_2 = 2$) and $N = 1$, in which the standard DMRG procedure with open boundary condition(OBC) is engaged.

We computed the ground state phase diagram of the

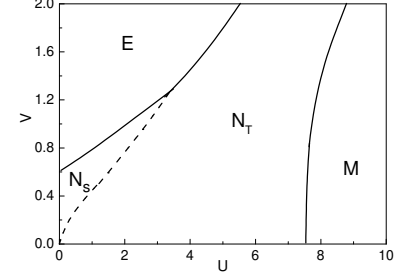


FIG. 2: The phase diagram of semiconducting SWCN(3,2). See the text for details.

intrinsic semiconducting SWCN (3,2)(see Fig.(2)). It can be divided into three phases as the *excitonic insulator*(E), *normal semiconductor*(N), and *Mott insulator*(M), which is in fact a result of the competition between the onsite(U) and the n.n.(V) Coulomb interactions. For our minimal model as Eq.(2) when both U and V are small, the system can be divided into two regions N_s and N_T , while V favors the former and U the latter. The ground state in any of the two regions is non-degenerate with its total spin equal to zero and no long range orders have been found in either charge or spin degree of freedoms. However, the first excitation in region N_s is a spin singlet state while the counterpart in the N_T region is spin triplet. Both the first excitations open a correspondent finite energy gap upon their own ground states. We interpret these excitations in connection with the singlet excitons as well as triplet ones for an intrinsic semiconducting SWCN system. The division line between N_s and N_T is shown as the dashed line in Fig.(2), across which a level crossing takes place for the gapful excited states with different spin symmetries. As a result, the calculated equal time correlation function (ETCF) for the ground state shows that the exponentially decaying staggered density-density ETCF is much stronger than the staggered spin-spin ETCF in the N_s region and vice versa in the N_T region. Therefore, these two regions should be identified as a onefold phase, i.e., normal semiconductor phase N .

If we still keep U small but increase V , the first spin singlet excitation would get lowered with the ground state density-density ETCF growing and extending. When it reaches the ground state, the system then undergoes a transition into a new phase in association with the excitonic insulator[19]. As a consequence of the “fallen state”, there are two mutually orthogonal degenerate ground states in the E phase as $|G_+^{(E)}\rangle$ and $|G_-^{(E)}\rangle$, in which the 2-fold degeneracy is understood in the thermodynamic limit. Both of them are spin singlet and are eigenstates of the parity, belonging to eigenvalue ± 1 , respectively. We stress that the completeness of state-counting from region N_s to phase E is preserved. More-

over, the density-density ETCFs of the two degenerate ground states are identical and no longer decaying. The amplitude of the ETCF increases with increasing V as shown in Fig.(3). Such a non-decaying correlation could be interpreted as the existence of a kind of long range order in the two ground states. To explore the nature of such long range order, we compute the matrix element of the site electron density n_m^ν in the subspace spanned by these two degenerate states. It is found that the diagonal term $\langle G_+^{(E)} | n_m^\nu | G_+^{(E)} \rangle$ (or $\langle G_-^{(E)} | n_m^\nu | G_-^{(E)} \rangle$) is trivially equal to 1, but the off-diagonal matrix element is

$$\langle G_+^{(E)} | n_m^\nu | G_-^{(E)} \rangle \sim (-1)^\nu \tilde{n} \quad (3)$$

with \tilde{n} being a site-independent constant and $(-1)^\nu = \pm 1$ for $\nu = A, B$, respectively. It shows a non-zero oscillation from A to B sublattices. This provides a strong evidence that the nature of long range order is of the charge density wave type. This also implies that the ground state subspace may accommodate such states with staggered density distribution referring to certain external constraints or environment.

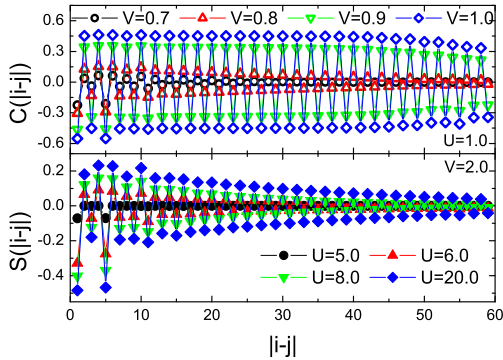


FIG. 3: The charge and spin correlation functions. The coordinate system for the horizontal axis is explained in Fig.(1c). The origin is set on the atom A in the middle cell of the tubule. The data are obtained by keeping 2000 states and with 1-2 finite size sweep to get convergent results. The upper panel gives the change of correlation $C(|i-j|)$ with respect to V for fixed $U = 1.0$ and the lower panel is the antiferromagnetic spin correlation $S(|i-j|)$ for different U with fixed $V = 2.0$.

Starting from the region N_T , if we further increase U , the triplet first excitation would be lowered continuously with the ground state spin-spin ETCF growing. In Fig.(3b), we show the variation of spin correlation versus U for fixed value of V . Until some critical value of $U = U_c$, the triplet spin gap vanishes in the thermodynamic limit[21], and a transition from phase N to the Mott phase M takes place. In the Mott phase, besides a finite charge gap the system develops gapless spin wave excitations. Since this part of phase diagram is far

from the possible realistic parameter region of U and V , in this paper, we shall not pay more attention to it.

The phase boundaries in Fig.(2) are determined by plotting the first excitation gap upon the ground state as the function of U with V being fixed which is actually computed in the particle hole channel. In this procedure, we adopt the infinite algorithm with 1000 states being kept and then extrapolate the finite size data to the thermodynamic limit. For $V = 2$ in Fig.(4a), the 2-fold de-

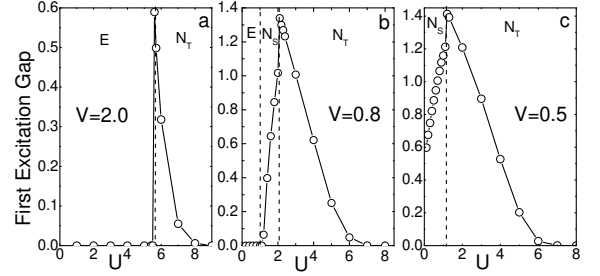


FIG. 4: The first excitation gap as a function of onsite Coulomb potential U . For $V = 2.0$ in (4a), at the transition point from phase E to N_T , the degeneracy of the ground state disappears suddenly accompanied with the appearance of a finite spin triplet gap which decreases with increasing U and vanishes at about $U = 8.8$. For $V = 0.8$ in (4b), as the system enters region N_s from phase E , the two degenerate singlet ground states split up with a gap opening gradually. The gapped first excitation transits from singlet into triplet when U exceeds the $N_s - N_T$ boundary. For $V = 0.5$ in (4c), there is only one continuous transition across the boundary between regions N_s and N_T . The vertical dashed lines indicate the transition points.

generacy of the ground states in E phase is lifted abruptly at the $E - N_T$ phase boundary $U_C = 5.6$ and a finite spin triplet excitation gap is opened. It decreases with increasing U and vanishes at about $U = 8.8$. Fig.(4b) with $V = 0.8$ shows a different picture. The singlet first excitation emerges gradually from zero at the $E - N_s$ phase boundary. The singlet excitation in N_s region and the triplet excitation in N_T region meet each other and form a cusp at the division line without discontinuity. It can be easily expected, the Fig.(4c) with $V = 0.5$ only shows a $N_s - N_T$ transition qualitatively the same as that in Fig.(4b). To further explore the nature of the above shown phase boundaries, and in particular, as an independent check, we introduce and compute the average of double occupancy and the n.n. density-density correlation over the ground state δ and ρ , respectively, as[20]

$$\begin{aligned} \delta &\equiv \partial E_{GS} / \partial U = (H_U / U L) \\ \rho &\equiv \partial E_{GS} / \partial V = (H_V / V L) \end{aligned} \quad (4)$$

in which E_{GS} is the ground state energy per site and the application of the Hellmann-Feynmann theorem is im-

plied. For fix $V = 2.0$ or 0.8 , the δ and ρ as functions of

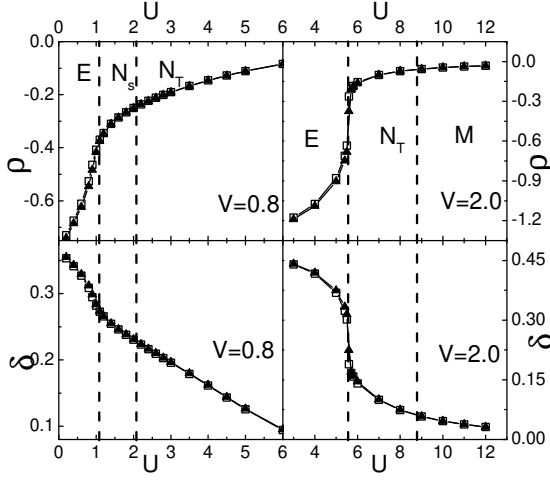


FIG. 5: The plot of δ and ρ as functions of U for fixed V . The vertical dashed lines indicate the transition points which are extracted from the phase diagram Fig.(2). The open squares and solid triangles are the data for 120 and 160 carbon atoms, respectively. In the right panel for $V = 2.0$, when U is increasing, a sharp change, i.e., a discontinuity, is found at the boundary from phase E to region N_T . The functional dependence across the $N_T - M$ phase boundary $U = 8.8$ is fairly smooth. In the left panel for $V = 0.8$, it shows that there is a discontinuity in the slopes of the δ and ρ as function of U on the $E - N_s$ phase boundary. In addition, the functional dependence across the $N_s - N_T$ boundary is also rather smooth where the level crossing of the first excitations takes place.

U are plotted in Fig.(5), respectively. The calculations are performed on the tubule with 120 and 160 carbon atoms by keeping 2000 states and sweeping 1-2 times to get convergent results. The results calculated from the 160 atoms coincide nicely with those from the 120 atoms, which provides a strong confidence that the calculated main features of the $N_s - E$ transition will survive in the thermodynamic limit. As shown in the right panel in Fig.(5), there is an abrupt jump for either δ or ρ at the critical point $V = 2.0$ and $U = 5.6$. It indicates the phase boundary between E and N_T belongs to the first order transition. If we further increase U from region N_T to phase M , the δ and ρ vary smoothly across the phase boundary (see also right panel of Fig.(5)). It is understood that the $N_T - M$ phase transition is of the Kosterlitz-Thouless type, where the N_T phase with a gapful (massive) triplet excitation spectrum transits into the M phase with spin wave type gapless (massless) excitations. In the left panel of Fig.(5), there is a discontinuity in the slope of both δ and ρ as functions of U on the $N_s - E$ phase boundary, which means this boundary belongs to a second order phase transition. In addition, it shows a smooth behavior in the functional dependence

of δ and ρ by the $N_s - N_T$ division line, which is consistent with the fact that N_s and N_T belong to the same phase N .

In our minimal model Eq.(1) and Eq.(2) the long range part of Coulomb interaction is ignored. Since we are dealing with the low energy excitations of the intrinsic semiconducting SWCN, the main effects of the long range Coulomb interaction could be confined in forming electron-hole pairwise excitations, and its remnant effect leads to a renormalization of U and V . Based upon such understandings we believe our minimal model is proper for the intrinsic semiconducting SWCN. Therefore, the physical ground state of the system under investigation lies in one of the three possible regions belonging to two phases as N_s , E or N_T , which provides a rich variety of experimentally measurable implications.

Acknowledgement: We thank sincerely to Profs. S.J.Qin, E.Tosatti, T.Xiang and L.Yu for beneficial discussions.

-
- [1] M. Bockrath, *et al.*, Nature(London) **397**, 598(1999)
 - [2] H. Ishii, *et al.*, Nature(London) **426**, 540(2003).
 - [3] L. Balents and M. P. A. Fisher, Phys. Rev. B **55**, R11973(1997)
 - [4] Yu. A. Krotov, D. H. Lee, and S. G. Louie, Phys. Rev. Lett. **78**, 4245(1997)
 - [5] C. Kane, L. Balents and M. P. A. Fisher, Phys. Rev. Lett. **79**, 5086(1997)
 - [6] M. J. O'Connell, *et al.*, Science **297**, 593(2002).
 - [7] S. M. Bachilo, *et al.*, Science **298**, 2361(2002).
 - [8] C. L. Kane and E. J. Mele, Phys. Rev. Lett. **90**, 207401(2003)
 - [9] C. D. Spataru, S. Ismail-Beigi, L. X. Benedict, and S. G. Louie, Phys. Rev. Lett. **92**, 077402(2004).
 - [10] H. Zhao and S. Mazumdar, Phys. Rev. Lett. **93**, 157402(2004)
 - [11] T. Ando, J. Phys. Soc. Jpn. **66**, 1066(1997).
 - [12] E. Chang, G. Bussi, A. Ruini, and E. Molinari, Phys. Rev. Lett. **92**, 196401(2004).
 - [13] M. P. Lopez Sancho, M. C. Munoz, and L. Chico, Phys. Rev. B **63**, 165419(2001)
 - [14] S. Saito, G. Dresselhaus and M. S. Dresselhaus, *Physical Properties of Carbon Nanotube*(Imperial College Press, London, 1998)
 - [15] W. A. Harrison, Phys. Rev. B **31**, 2121(1985).
 - [16] Andrei L. Tchougreeff and R. Hoffmann, *et al.*, J. Phys. Chem. **96**, 8993(1992).
 - [17] S. R. White, Phys. Rev. Lett. **69**, 2863(1992); Phys. Rev. B **48**, 10345(1993); U. Schollwöck, cond-mat/0409292
 - [18] C. T. White, D. H. Robertson, and J. W. Mintmire, Phys. Rev. B **47**, R5485(1993)
 - [19] D. Jerome, T. M. Rice, and W. Kohn, Phys. Rev. **158**, 462(1967)
 - [20] E. Jeckelmann, Phys. Rev. Lett. **89**, 236401(2002)
 - [21] The finite size algorithm with 2000 states kept is used to calculate the spin gap in the particle-hole channel up to 200 carbon atoms in the Mott phase. The gap value extrapolated to the thermodynamic limit is around \sim

10^{-4} , which can be viewed as zero.